Supramolecular Assemblies of Diacetylenic Aldonamides

David A. Frankel and David F. O'Brien*

Contribution from the C. S. Marvel Laboratories, Department of Chemistry, University of Arizona, Tucson, Arizona 85721

Received March 28, 1994®

Abstract: The study of novel amphiphiles that form nonspheroidal assemblies upon hydration is fundamental to understanding the relationship between molecular structure and supramolecular morphology. Structural components of previously reported amphiphiles were used to design the single chain diacetylenic aldonamides reported here. Open chain sugar headgroups were linked via an amide bond to a hydrophobic tail. Diacetylenes were incorporated in the alkyl chain both as a structural component and as a reactive unit. Photopolymerization was used to test the molecular ordering of the hydrophobic region of the assemblies and to enhance their thermal and chemical stability. The electron density of the diacetylenes allowed direct imaging of the assemblies by TEM. The morphology and reactivity of a series of *N*-dodeca-5,7-diynylaldonamides were determined. The aldonamides were derived from two aldoheptoses, D-glycero-D-gluconamide and D-glycero-L-mannonamide; four aldohexoses, D-galactonamide, D-gluconamide, L-mannonamide, and D-gulonomide; two aldopentoses, L-arbanonamide and L-lyxonamide; and two aldotetroses, L-threonamide and D-erythronamide. *N*-Dodecylaldonamide analogues were prepared and examined to evaluate the importance of the diacetylene group on the morphology. The microscopy and molecular modeling data indicate that at least two packing arrangements for these assemblies are possible. One is the head-to-head bilayer packing typical of most amphiphilic molecules; the other is a head-to-tail arrangement. The head-to-head packing results in assemblies which are planar, helical, or tubular. The head-to-tail packing arrangement and "dromic" hydrogen-bonding patterns are associated with fiber-like supramolecular assemblies. Numerous potential applications of tubule microstructures have been proposed. The relative ease of preparation of many of these aldonamide molecules and their assemblies recommends them for many of these applications.

Introduction

Membrane vesicles (liposomes) have been an active area of research since the 1960's. These spheroidal membranes are composed of amphiphilic bilayers that enclose an aqueous volume. Liposomes have proven useful as biological membrane models,[1] for the controlled delivery of chemical and biological therapeutic agents,[2,3] and for the photoinduced separation of charges and charged species.[4,5] A somewhat surprising development in recent years was the observation that certain amphiphiles form nonspheroidal assemblies upon hydration. These novel materials are fundamentally important as an aid to understanding the relationship between molecular structure and supramolecular morphology and as an opening to the preparation and utilization of nanoscale materials.[6]

By the mid 1980's, certain classes of amphiphilic compounds were reported to exhibit nonspheroidal supramolecular morphologies at temperatures below their corresponding main phase transition, T_m.[7-9] One class of amphiphiles, originally described by Yager and Schoen,[7] are double chain glycerol-based phosphatidylcholines (PC) which contain diacetylenes in both alkyl chains. When hydrated above their T_m they formed liposomes. However, in contrast to most PCs the liposomes were converted into helical and tubular supramolecular morphologies upon cooling below T_m.[10,11] Hydrated saturated analogs of the lipids formed liposomes both above and below the T_m. Equimolar mixtures of the *R* and *S* diacetylenic lipid ($DC_{8,9}PC$) exhibited only liposomal morphologies at all temperatures.

A second class of amphiphiles based on amino acid backbones, e.g., glutamic or aspartic acid, had the lipid tails attached to the two carboxyl moieties and the headgroup associated with the amino group.[12] The hydrophilic headgroup, a cationic quaternary ammonium, was linked to the backbone by a methylene spacer. The study demonstrates the utility of intermolecular amide hydrogen bonding for the formation of a nonspheroidal morphologies. When the methylene spacer was short ($n < 10$), the bulky headgroup appeared to interfere with efficient intermolecular hydrogen bonding and only liposomes were observed at all temperatures. In contrast, helical and tubular supramolecular morphologies were observed at temperatures below the T_m when the spacer was longer than 10 methylenes. Ihara and co-workers found that glutamate lipids having two alkyl chains connected to the backbone via amide bonds formed helical bilayer assemblies,[13,14] whereas hydration of the corresponding ester glutamate lipids produced liposomes. Photopolymerizable analogs of the amide glutamate lipids formed helical microstructures as well.[15]

Single chain alkyl aldonamides, which consist of an open chain hexose headgroup linked to a saturated alkyl chain through an amide bond, were described by Pfannemüller and Welte[8] and

* Abstract published in *Advance ACS Abstracts*, September 15, 1994.

(1) Bangham, A. D.; Hill, M. W.; Miller, N. G. A. *Methods in Membrane Biology*; Plenum Press: New York, 1974; Vol. 1.
(2) Lamparski, H.; Liman, U.; Barry, J. A.; Frankel, D. A.; Ramaswami, V.; Brown, M. F.; O'Brien, D. F. *Biochemistry* **1992**, *31*, 685–694.
(3) Papahadjopoulos, D. *Ann. N. Y. Acad. Sci.* **1978**, *308*, 1–462.
(4) Armitage, B.; O'Brien, D. F. *J. Am. Chem. Soc.* **1992**, *114*, 7396–7403.
(5) Robinson, J. N.; Cole-Hamilton, D. J. *Chem. Soc. Rev.* **1991**, *20*, 49–94.
(6) Whitesides, G. M.; Mathias, J. P.; Ceto, C. T. *Science* **1991**, *254*, 1312–1319.
(7) Yager, P.; Schoen, P. E. *Mol. Cryst. Liq. Cryst.* **1984**, *106*, 371–381.
(8) Pfannemuller, B.; Welte, W. *Chem. Phys. Lipids* **1985**, *37*, 227–240.
(9) Nakashima, N.; Asakuma, S.; Kunitake, T. *J. Am. Chem. Soc.* **1985**, *107*, 509–510.
(10) Yager, P.; Schoen, P. E.; Davies, C.; Price, R.; Singh, A. *Biophys. J.* **1985**, *48*, 899–906.
(11) Georger, J.; Price, R.; Singh, A.; Schnur, J. M.; Schoen, P. E.; Yager, P. *J. Am. Chem. Soc.* **1987**, *109*, 6169–6175.
(12) Nakashima, N.; Asakuma, S.; Kim, J.-M.; Kunitake, T. *Chem. Lett.* **1984**, 1709–1712.
(13) Ihara, H.; Fukamoto, T.; Hirayama, C.; Yamada, K. *Polym. Commun.* **1986**, *27*, 282–285.
(14) Ihara, H.; Yamaguchi, M.; Takafuji, M.; Hachisako, H.; Hirayama, C.; Yamada, K. *Nippon Kagaku Kaishi* **1990**, 1047.
(15) Ihara, H.; Takafuji, M.; Hirayama, C.; O'Brien, D. F. *Langmuir* **1992**, *8*, 1548–1553.

0002-7863/94/1516-10057$04.50/0

later by Führhop and co-workers.[16,17] Variation of the alkyl chain length (between 8 and 16 carbons) had little effect on the assembly morphology whereas alteration of the sugar headgroup resulted in several unusual supramolecular morphologies. These aldonamides, unlike typical surfactants, were not very water soluble and could only be readily hydrated at elevated temperatures producing micellar structures. When micellar solutions of hexose aldonamides, i.e., galactose, glucose, mannose, gulose, and talose, were cooled they reorganized into nonspheroidal assemblies.[17]

Archibald and Yager reported that thermal cycling of suspensions of nonhydroxy cerebrosides or α-hydroxy cerebrosides produced helical bilayer or tubular microstructures, respectively.[18]

The important structural components of the previously reported amphiphiles were used to design the novel diacetylenic aldonamides reported here. The amphiphile is a single chain nonionic surfactant that is conveniently synthesized. Open chain sugars were used as headgroups and linked to the tail by an amide bond which has been shown to be an effective structural component for the formation of nonspheroidal morphologies. Finally, diacetylenes were incorporated in the alkyl chain for four reasons. First, the rigid diacetylene unit was an important structural component in the formation of the tubular and helical morphologies from the diacetylene phosphatidylcholines. Second, diacetylenes polymerize in a topotactic fashion, to form a highly conjugated eneyne backbone that absorbs in the visible spectral region. This reaction of the diacetylenes can be used to test the molecular ordering of the hydrophobic region of the assemblies. Third, the electron density of the diacetylenes allows direct imaging of the assemblies by TEM without the addition of heavy metal stains which sometimes create sample artifacts. Finally, once the assemblies were formed, the polymerization of the diacetylenes enhanced the thermal and chemical stability of the assemblies by the covalent association of the amphiphiles.

Experimental Section

Aldonamide Synthesis. The synthesis and spectral characterization of the diacetylenic and saturated aldonamides are available in the supplemental material.

Formation Of Supramolecular Assemblies. Diacetylenic Aldonamides. The weighed diacetylenic aldonamides were placed in a glass test tube with Milli-Q water which was measured and distributed by Eppendorf micropipets. The insoluble samples were carefully heated to a boil with a heat gun. At ca. 100 °C the aldonamide solutions were clear. The solutions were allowed to cool to rt. Rates of cooling varied from 10 °C/h to rapid cooling of the solution in ice–water. No visible difference in the supramolecular assemblies was observed by altering the rate of cooling. Sample preparation was easily reproduced several times. The supramolecular assemblies formed as the solutions cooled through the temperature region associated with their phase transition. The solution concentrations varied from 0.0125 mg/mL to 3 mg/mL (aldonamide/water). The assemblies eventually precipitated from solution and were used without further preparation.

Saturated Aldonamides. Assemblies of the saturated aldonamides were prepared in an analogous fashion to the diacetylenic aldonamides. The samples were weighed, dissolved in boiling Milli-Q water, and cooled to rt. Since the L- and D-galactonamides were practically insoluble even in boiling water, the clear aqueous solution was decanted from the residual undissolved material and then cooled to yield a limited number of precipitated aggregates. The L-mannonamide was the next least soluble aldonamide. The boiling aqueous solution was also decanted from the undissolved material and allowed to cool to rt to form the assemblies. The D-gluco, D-gulo, L-arabino, and L-lyxono aldonamides were all very soluble in boiling water and upon cooling formed a gelatinous network. The four carbon sugars were slightly soluble in aqueous solution, and small aggregates were visible when the solution cooled to rt. The solution concentration varied from 50 mg/mL to less than 1 mg/mL (aldonamide/water).

Polymerization of Aldonamides. The samples were placed in quartz cuvettes and capped. The thermostated samples (25 °C) were irradiated with a low-pressure mercury lamp (254 nm) from a distance of 1–4 cm. Irradiation times varied up to 60 min.

Transmission Electron Microscopy (TEM). Preparation of TEM Grids. Copper grids (300 Mesh, Ted Pella Co., Tustin, CA) were cleaned by ultrasonication, dried, and then coated with a solution of Formvar or Pioloform. A thin layer of carbon (<1 nm) was then deposited on the coated grid. The grid surface was made hydrophilic by either UV irradiation or by a glow-discharge treatment in an argon atmosphere.

Sample Preparation. The grids were dipped into hot aqueous solutions or into the aggregate suspensions. Both methods produced similar results and only the latter was used extensively. The grids were placed on filter paper and dried overnight in a clean container. The diacetylenic aldonamides were used without further preparation. The saturated aldonamides were negatively stained with either 0.5% phosphotungstic acid (PTA) or 0.5% uranyl acetate (UA) in Milli-Q water (pH adjusted to 7.0). A drop of stain was applied to the sample and immediately wicked away with a piece of filter paper. The sample was air dried from 30 min to 16 h. Some samples were also observed by platinum shadowing at an angle of 35°. Reproducible samples were observed, and representative micrographs are shown.

TEM Microscopy. Microscopy was conducted on a Hitachi H-500 TEM. The accelerating voltage was 75 keV, condenser aperture 300 or 400 μm, objective aperture 20 or 30 μm, spot size 10 μm, and beam current 15 mA. The TEM images were captured on electron microscope film (Kodak) and developed with Dektol.

Optical Microscopy. Glass microscope slides were ultrasonically cleaned with water and dried with a lens tissue. A drop of the aldonamide solution was placed on the slide, covered with a cover slip, and examined with a Hamamatsu Video Camera Model 2400 attached to a Zeiss Axioplan microscope. Image processing was performed with Image-1 Software by Universal Imaging Corporation. The scale was calibrated using a micrometer slide at each objective magnification. Images were saved as TIFF files and output to hard copies via a film recorder.

Molecular Modeling. Molecular modeling of the aldonamides was performed on a Silicon Graphics Iris Work Station using Sybyl Molecular Modeling Software v 6.0 (TRIPOS Associates, Inc., St. Louis, MO). The extensive number of possible conformations of each of the sugar headgroups was reduced by initially restricting the conformation to that of the X-ray crystallographic structure of the corresponding sugar alditol. X-ray structures of the alditols were obtained from the Cambridge X-ray crystallographic database and imported directly into Sybyl. The terminal carbon of the alditol was deleted, and the diacetylenic amide chains were attached. The aldonamide was then minimized (Tripos/Force field method) to correct for bond or angle irregularities caused by the modifications described above. An extensive search of the crystallographic database[19] indicated that the common packing of aldonamides as well as diacetylenes is monoclinic ($a \neq b \neq c$, $\alpha = \gamma = 90°$, $\beta \neq 90°$) or triclinic ($a \neq b \neq c$, $\alpha \neq \beta \neq \gamma \neq 90°$) rather than hexagonal or cubic. Therefore, the amphiphiles were arranged in a 2 × 2 lattice. The aldonamide molecule was copied with one molecule labeled as the ligand and the other as the site. The formal charges were calculated by the Gasteiger–Hückel method. The two molecules were brought together minimizing the intermolecular interaction energy between the two molecules (electrostatic, hydrogen bonding, and van der Waals). The lattice was expanded to 2 × 2 by repeating the procedure. The 2 × 2 lattice was then minimized by the Tripos force field and possible hydrogen bonding was visualized. The saturated L-arabonamide was modeled in a similar fashion except the attached chains were saturated.

Results

Aldonamide Synthesis. Diacetylenic chains derived from *N*-dodeca-5,7-diyn-1-amine were used in all the diacetylenic syntheses. The alkynyl proton of 1-hexyne was deprotonated with an ethyl Grignard and subsequently exchanged with iodine to form the 1-iodoheyne in quantitative yield. The iodohexyne was oxidatively coupled to 5-cyano-1-pentyne using a modified Cadiot–Chodkewicz method to give the diacetylenic nitrile.[20] The

(16) Fuhrhop, J.-M.; Schnieder, P.; Rosenberg, J.; Boekema, E. *J. Am. Chem. Soc.* **1987**, *109*, 3387–3390.
(17) Fuhrhop, J.-H.; Schnieder, P.; Boekema, E.; Helfrich, W. *J. Am. Chem. Soc.* **1988**, *110*, 2861–2867.
(18) Archibald, D. D.; Yager, P. *Biochemistry* **1992**, *31*, 9045–9055.
(19) Allen, F. H.; Davies, J. E.; Galloy, J. J.; Johnson, O.; Kennard, O.; Macrae, C. F.; Mitchell, E. M.; Mitchell, G. F.; Smith, J. M.; Watson, D. G. *J. Chem. Inf. Comp. Sci.* **1991**, *31*, 187–204.
(20) Frankel, D. A.; O'Brien, D. F. *J. Am. Chem. Soc.* **1991**, *113*, 7436–7437.

Table 1. Optical Activity of Monomer Solutions[a] and Supramolecular Morphology of Hydrated *N*-Dodeca-5,7-diynyl Aldonamides and *N*-Dodecylaldonamides

	N-dodeca-5,7-diynyl-		*N*-dodecyl-	
headgroups	$[\alpha]_D$ (deg)	morphology	$[\alpha]_D$ (deg)	morphology
L-arabinose	+33.3	braided fibers	+30.4	helices and tubules
D-galactose	+28.3	helices and tubules	+23.4	helices and tubules
D-glucose	+34.3	sheets	+27.1	braided fibers
D-glycero-D-glucose	+15.0	sheets	NA	NA
D-glycero-L-mannose	+12.0	helices and tubules	NA	NA
D-glucose	+15.8	tubules	+14.6	sheets
L-lyxose	+23.0	open and closed tubules	+17.8	open and closed tubules
L-mannose	+16.0	tubules	+14.8	helices and tubules
L-threose	+36.6	sheets	+38.0	sheets

[a] Optical rotations were determined for aldonamide solutions in DMSO at 23 °C and are reported for 1 g/mL concentration.

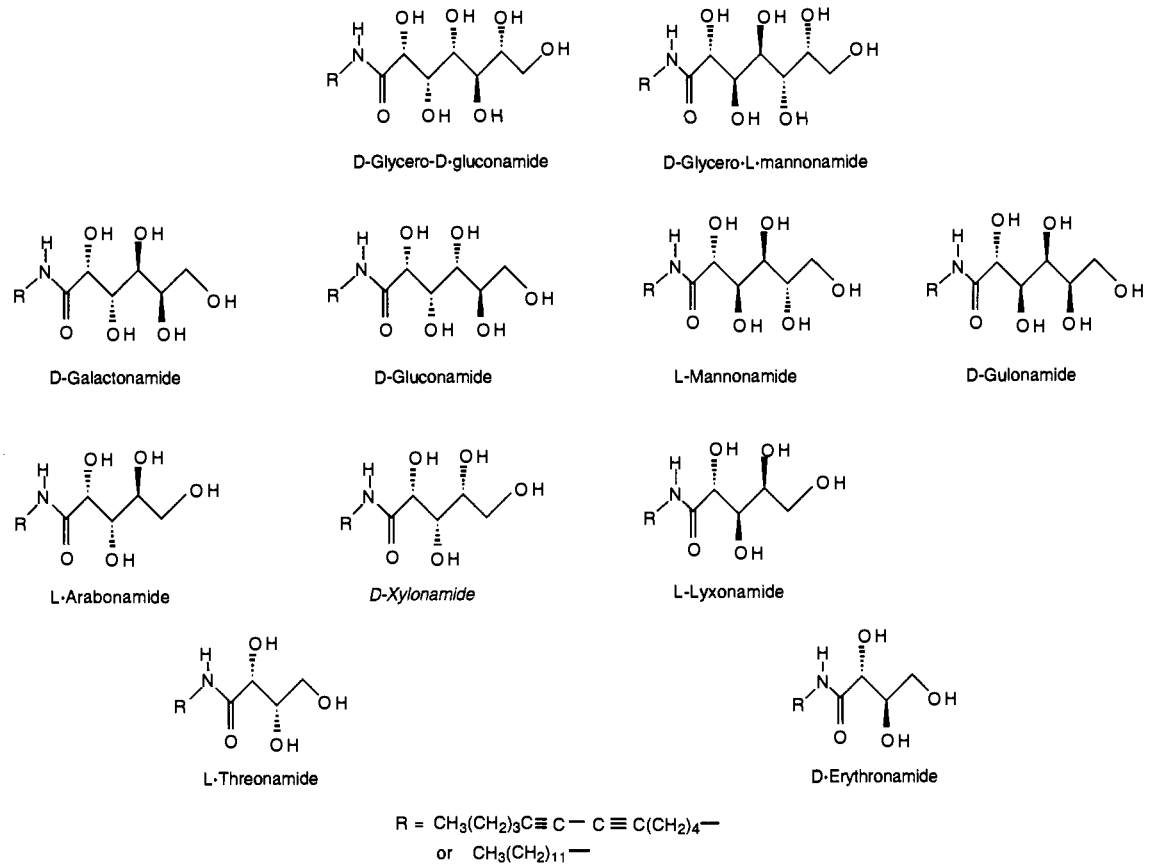

Figure 1. Aldonamide chemical structures.

nitrile moiety was reduced with lithium aluminum hydride to the amine without perturbation of the diacetylene.

The fatty amine was coupled to the sugar headgroups using several synthetic strategies. The fatty amine was refluxed in methanol with the commercially available 1,4-γ-lactone sugars to give the aldonamide products. When the lactone sugars were unavailable the reducing sugars were oxidized by one of two techniques. Bromine/water oxidation of the reducing sugar gave the aldonic acid, which was converted to the methyl ester and then reacted with the diacetylenic amine to give the desired product. However, the acidic oxidation conditions were too harsh for L-lyxose; therefore, a basic oxidative approach was adopted. The reducing sugar was treated with *in situ* generated hypoiodite. The resulting ionized acid was converted to the hemicalcium salt by the addition of $CaCl_2$. This insoluble salt was mixed with an acidic ion-exchange resin, in methanol. After evaporation of the solvent, the 1,4-γ-lactone of the sugar was isolated and then refluxed with the fatty amine to give the lyxonamide product. In the last strategy, the hemicalcium salt of L-threose was treated with Amberlite in methanol. Upon solvent evaporation the methyl ester was isolated and then refluxed with the diacetylenic amine to yield the aldonamide.

The synthesis of the saturated aldonamides was accomplished in the same manner as the diacetylenic aldonamides except that dodecylamine was used. Saturated analogs of all the diacetylenic aldonamides were prepared with the exception of the heptose aldonamides.

The optical activity of each aldonamide monomer was determined in DMSO solution at 23 °C, and they are reported in Table 1 at a standard 1 g/mL concentration.

Supramolecular Diacetylenic Aldonamides Assemblies. The structures of the diacetylenic aldonamides prepared for this study are shown in Figure 1. The four aldohexoses, D-galactonamide, D-gluconamide, L-mannonamide, and D-gulonamide, were originally described in a preliminary paper[20] which appeared simultaneously with an independent report on the D-gluconamide.[21] Each of these aldonamides has the same stereochemistry at the chiral carbon adjacent to the amide carbonyl. Since the

(21) Fuhrhop, J.-M.; Blumtritt, P.; Lehmann, C.; Luger, P. *J. Am. Chem. Soc.* **1991**, *113*, 7437–7439.

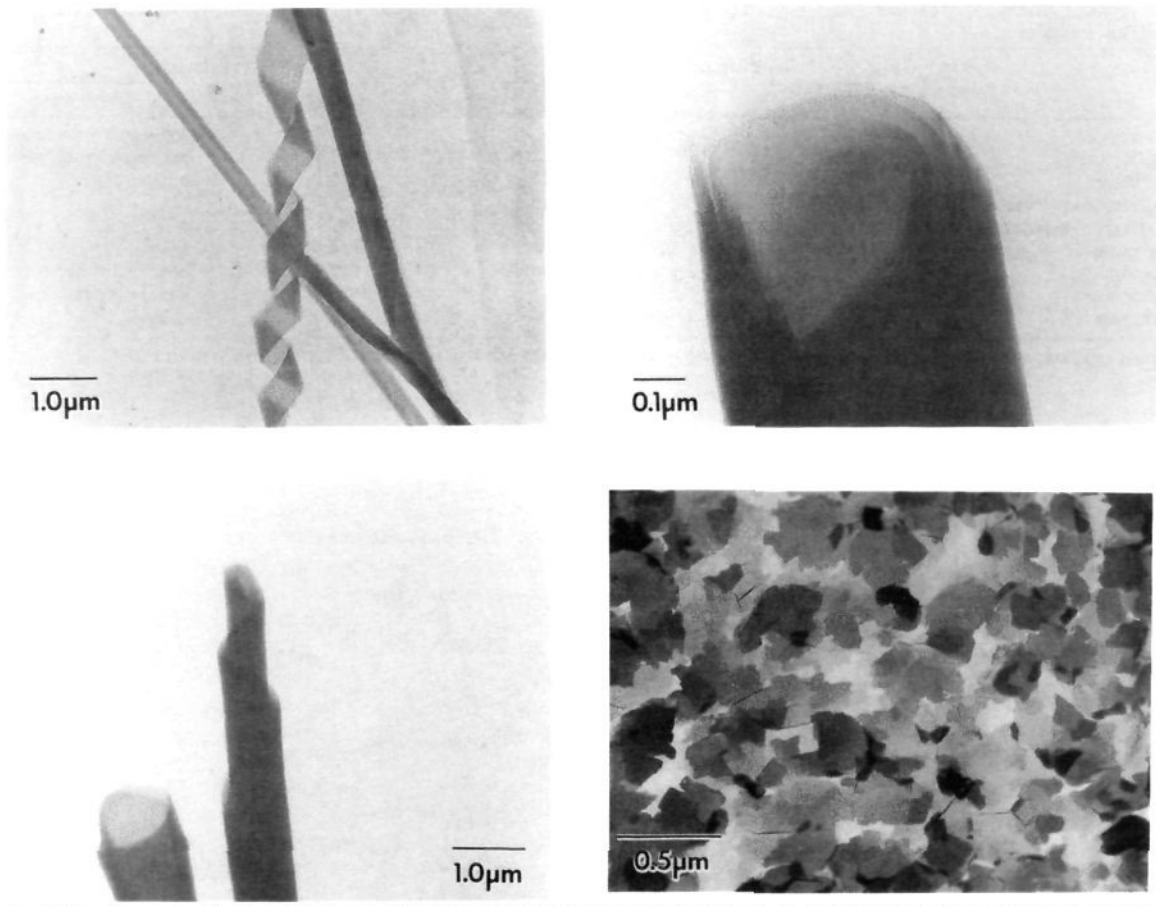

Figure 2. TEMs of unstained hydrated *N*-dodeca-5,7-diyne galactonamide assemblies. (Top left) right-handed helical and tubule structures from *N*-dodeca-5,7-diynyl D-galactonamide (1.0 mg lipid/mL water). (Top right) end-on view of a hollow polymerized tubule from *N*-dodeca-5,7-diynyl D-galactonamide after treatment with formamide 1:1 (1.0 mg lipid/mL water). (Bottom left) assemblies of *N*-dodeca-5,7-diynyl L-galactonamide showing its left-handed nature (1.0 mg lipid/mL water). (Bottom right) planar assemblies formed from a 1:1 racemic mixture of *N*-dodeca-5,7-diynyl D- and L-galactonamides (1.0 mg lipid/mL water).

D,L nomenclature convention for aldoses designates the configuration at the carbon adjacent to the terminal primary alcohol, i.e., the opposite end of the carbohydrate part of the molecule, some of the compounds in Figure 1 are D and others are L. The columns in Figure 1 show variation in the aldose (headgroup) size, and the rows show the variation in stereocenters examined.

These diacetylenic amphiphiles, unlike typical surfactants, are very insoluble in water and can only be hydrated to form supramolecular assemblies at elevated temperatures near 100 °C. Saturated aldonamides were shown to form micelles at these temperatures.[8] Other amphiphilic molecules that form non-spheroidal morphologies exhibit a transition from liposomes or micelles to a structure that is tubular or helical in nature.[10,16,17] When solutions of diacetylenic aldonamides were cooled aggregates of the amphiphiles began to precipitate. The supramolecular assemblies formed by this process could subsequently be directly visualized by TEM, taking advantage of the electron density of the diacetylene or polydiacetylene.

Enantiomeric Effect. The D-galactonamide forms hollow tubules as seen in Figure 2. The hollow tubules average 0.31 ± 0.09 μm in diameter with an average aspect ratio of ca. 10. About 5% of assemblies observed in the TEMs appear as helical ribbons (Figure 2 (top left)). The amphiphiles appear to form bilayer sheets that twist due to the intrinsic curvature of the enantiomerically pure amphiphiles.[22] The helical structure can wind tighter to form closed tubules as seen on the right side of Figure 2 (top left). The outside of some tubules shows the helical marking of their likely precursors. The open end of the tubules shows several bilayers that are wrapped around a central aqueous core (Figure 2 (top right)). The thickness of each sheet is ca. 3.5 nm which is reasonable for a galactonamide bilayer.

Since enantiomers exhibit the same physical properties, the D- and the L-galactonamide was expected to form similar assemblies. Indeed, they both form hollow tubules. Figure 2 (top left) shows a D-galactonamide assembly with an open helical portion. The micrograph shows that the helix is turning from left to right and is noted as right-handed. Figure 2 (bottom left) displays a hollow tubular assembly with a left-handed orientation formed from the L-galactonamide amphiphile. When equimolar amounts of the D- and L-galactonamide were mixed and hydrated in water to form supramolecular assemblies, only flat planar platelets were observed (Figure 2 (bottom right)). An explanation for these observations may be found in the previously proposed chiral bilayer effect.[16] An enantiomerically pure aldonamide, when hydrated at high temperatures, forms chiral micelles. Upon cooling, these chiral micelles rearrange to chiral bilayers in which all the amphiphiles are packed with the same orientation. This causes the bilayer to twist, resulting in the observed morphologies. On the other hand, a mixture of both the D- and L-enantiomers yields racemic micelles in which the enantiomers may be paired. Upon conversion to bilayers, the racemic or paired amphiphiles form achiral structures as observed.

Variation of Headgroup Size. Three series of aldonamides were synthesized to investigate the effect of altering the balance between hydrophilic/hydrophobic regions in the molecule on the morphology of the assemblies. This could be accomplished by either altering the alkyl chain length or the headgroup size relative

(22) Helfrich, W. J. *J. Chem. Phys.* **1986**, *85*, 1085–1087.

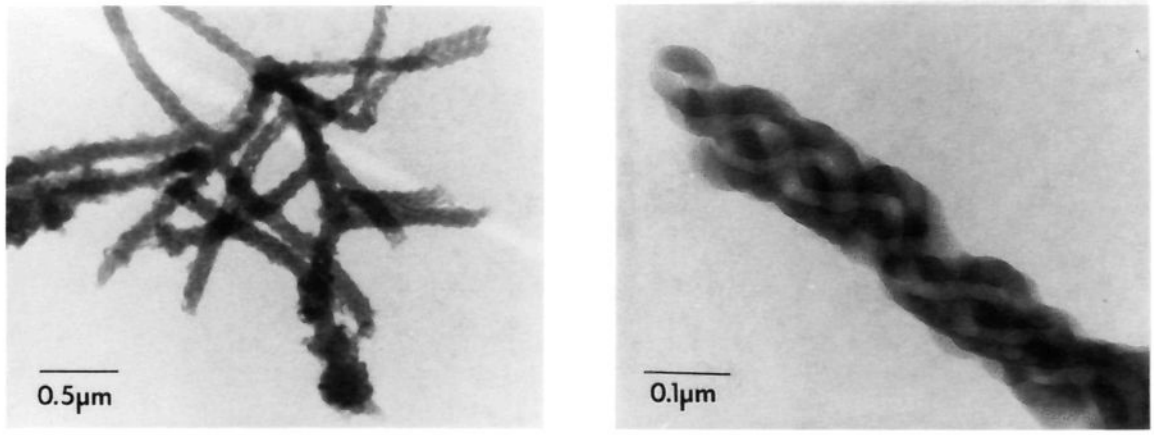

Figure 3. (Left) TEMs of unstained hydrated *N*-dodeca-5,7-diynyl L-arabonamide assemblies. Braided fibers of *N*-dodeca-5,7-diynyl L-arabonamide (1.0 mg lipid/mL water). (Right) the same structure at higher magnification which suggests the assembly is composed of four individual strands.

to the other component of the amphiphile. Increasing the alkyl chain length changes the T_m of the amphiphile, but was reported to have little effect on the supramolecular morphology.[8,16] On the other hand, we observed that altering the headgroup dramatically affects the supramolecular morphology. Aldonamides with headgroups composed of open chain sugars having seven, six, five, or four carbons were prepared (Figure 1). Each series was named for the aldonamide with the largest headgroup.

D-Galactose Series. All the aldonamides in the D-galactose series exhibit quite different supramolecular morphologies as the size of the headgroup size varied. The first aldonamide in this series, D-galactose (Figure 2, discussed above), forms hollow tubular assemblies. The five-carbon sugar, L-arabonamide, shows a strikingly different morphology when dispersed in water (Figure 3 (left)). The twisted helical assembly appears to be composed of several individual fibers or strands that are braided together or twisted until they kink back on themselves like a garden hose (Figure 3 (right)). The overall diameter (0.12 μm) of the braided structures is somewhat smaller than that of the D-galactonamide tubules. The individual strands that compose the braided fibers have a diameter of ca. 30 nm, indicating they are composed of several layers of amphiphiles. The TEM data suggest that the helical assembly is a consequence of the intertwining of four strands. The L-threonamide is the tetrose for both this series and the D-glycero-D-glucose series and is discussed below.

D-Glycero-D-glucose Series. The seven-carbon D-glycero-D-gluconamide forms planar sheets when hydrated in water. These sheets are stacked multilayers with an aspect ratio (length/width) of ca. 5 (Figure 4 (top left)). The six-carbon D-gluconamide, also forms multilayered sheets (Figure 4 (top right)). The sheets do not show a tendency to roll up to form tubular assemblies. The D-gluconamides are the only hexose aldonamide examined which formed planar assemblies. Figure 4 (top right) shows the planar sheet morphology of D-gluconamide which exists as stacks of several layers. It is possible that the packing arrangement of the amphiphiles in the bilayer sheets induces a net dipole along the planar sheet. Other layers with dipoles in the opposite direction would then associate with the surfaces to form the stack. The smallest aldonamide in this series, the L-threonamide, forms similar sheetlike structures. L-Threonamide, when hydrated in water, gives flat planar structures (Figures 4 (bottom left and bottom right). The rectangular assemblies are 0.5 μm thick which corresponds to ca. 200 monolayers. The assemblies appear more crystalline than the other planar morphologies. The surface markings in the optical micrograph could be due to elevation defects. The corresponding five-carbon sugar, D-xylose, was not synthesized.

D-Glycero-L-mannonamide Series. The D-glycero-L-mannonamide and L-mannonamide form similar tubular structures when hydrated in water. Figure 5 shows the tubular and helical ribbon morphologies of the heptose aldonamide. About 50% of the structures observed in the TEMs were helical ribbons which probably wind up to form the hollow tubules. The tubules have an average length of 9.2 ± 0.25 μm with diameters of 0.30 ± 0.1 μm. The helical ribbons that form the tubules are 0.63 ± 0.05 μm in width, or about twice the diameter of the tubule. The tubules can also be observed in an aqueous solution via optical microscopy (Figure 5 (top right)).

The removal of one carbon from the sugar headgroup gives the L-mannonamide, which generally forms hollow tubular assemblies similar to that of D-galactonomide (Figure 5 (bottom left and bottom right)). The hollow aqueous core of this assembly is seen by the light area which runs the entire length of the tubule. The L-mannonamide tubules average 0.37 ± 0.1 μm in diameter and have an average length of 2.9 ± 0.3 μm. The thickness of the sheets which make up the tubules was estimated to be 3 nm from end-on micrographs of the assemblies. This value is consistent with a bilayer arrangement of the amphiphiles. Helical structures were not observed in the TEMs.

Hydration of the pentose aldonamide, L-lyxose, results in the formation of tubules and partially unwound sheets as seen in Figure 6. The tubules have average diameters of 0.27 ± 0.09 μm with lengths of ca. 6 μm. The tubules appear to be formed by the rolling up of bilayer or multilayer sheets. About 50% of the assemblies observed in TEMs were unwound. The sheets have average widths of 0.89 μm.

Finally, the morphology of the tetrose aldonamide, D-erythronamide, is quite different from the other aldonamides in this series. The usual tubular morphology was no longer present; instead, a random network of small fibers was observed (not shown). Although the fibers were observed to be several μm in length, the image resolution was insufficient to determine whether the fibers were solid or hollow.

D-Gulonamide. The D-gulonamide also forms tubular assemblies which appear to consist of small fibers that wrap or twist around each other in a helical array to form larger tubular assemblies. Figure 7 shows the ends of the smaller tubular structures which make up the assembly. These micrographs show the overall open tubular morphology of the system as well as the substructures. The average diameters of these tubular structures is 0.37 ± 0.15 μm.

Saturated Aldonamide Assemblies. The aldonamides associate through a delicate balance of forces. A comparison of the supramolecular morphologies of the diacetylenic and saturated aldonamides should aid in understanding the dominant forces. The formation of different supramolecular morphologies upon hydration of the diacetylenic and saturated aldonamides indicates that interactions between the acyl tails and π-orbital overlap of the diacetylenes are the predominant forces. In contrast, the formation of similar morphologies indicates that the headgroup

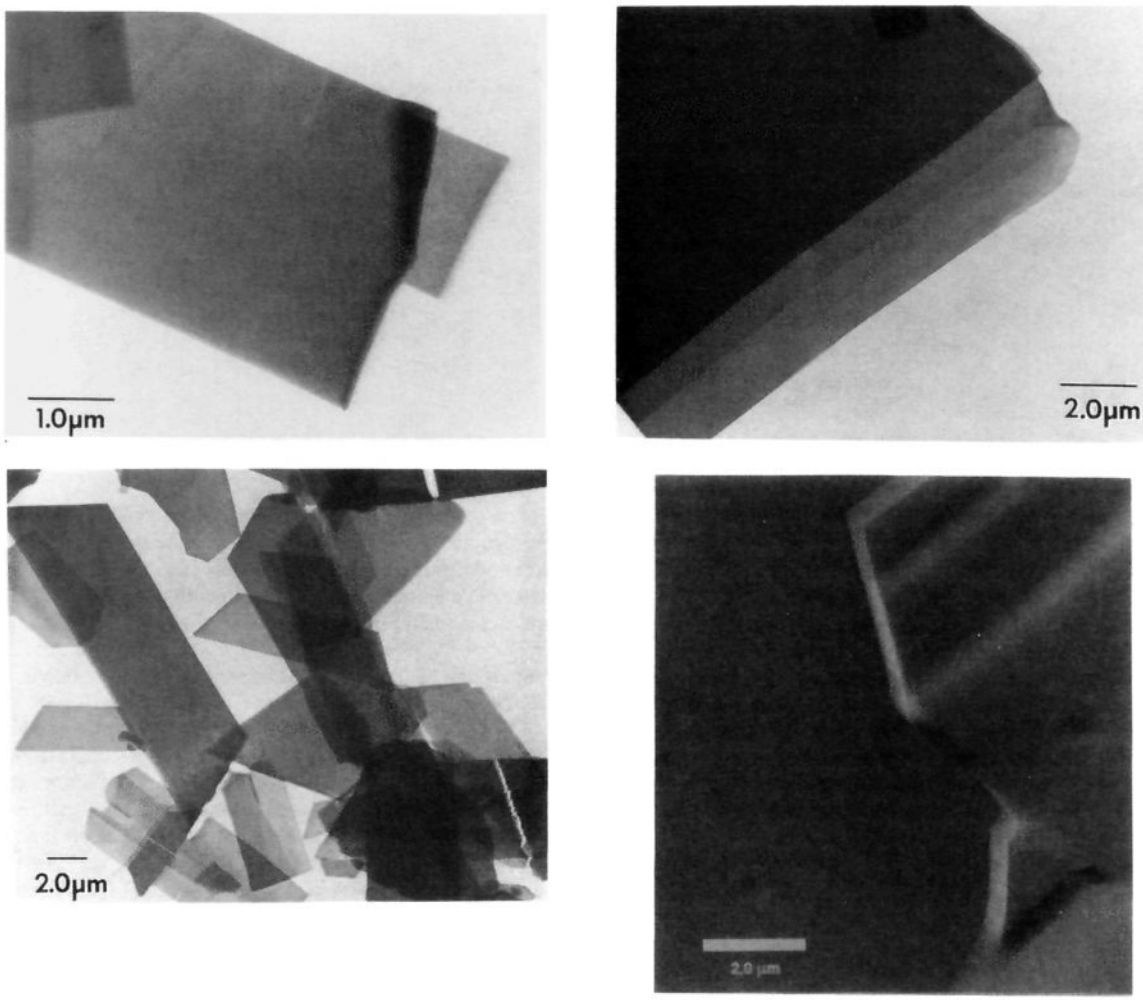

Figure 4. (Top left) TEM of unstained hydrated assemblies of *N*-dodeca-5,7-diynyl D-glycero-D-gluconamide (1.0 mg lipid/mL water). (Top right) TEM of *N*-dodeca-5,7-diynyl D-gluconamide assemblies show planar sheets (1.0 mg lipid/mL water). (Bottom left) TEM of planar assemblies of *N*-dodeca-5,7-diynyl L-threonamide (1.0 mg lipid/mL water). (Bottom right) video-enhanced optical micrography of *N*-dodeca-5,7-diynyl L-threonamide assemblies (1.0 mg lipid/mL water).

packing and the hydrogen bonding dominate the amphiphilic association. Therefore, a simple change in the tails of the amphiphile is a useful method of probing the relative influences of these noncovalent interactions on the overall supramolecular morphology.

Since increasing the methylene spacer length of amphiphiles has been shown to have little effect on the supramolecular morphology of these systems,[8] we examined the chain packing effect of the amphiphiles by replacing the dodeca-5,7-diyne unit with a dodecyl group. The absence of the diacetylene group made it necessary to use negative staining or platinum shadowing of the samples to visualize the assemblies by TEM.

The morphologies of the supramolecular assemblies formed from the *N*-dodecyl aldonamides were similar to those of the diacetylenic aldonamides in approximately half of the cases (Table 1). The *N*-dodecyl D-galactonamide yields tubular assemblies and some helical ribbon structures (Figure 8). The diameters of the tubules average 1.0 μm and the helical ribbons are nearly that same size (0.78 μm). The diacetylenic D-galactonamide tubules were about one-third the diameter and length of the saturated D-galactonamide.

The *N*-dodecyl-L-mannonamide also forms hollow tubular assemblies when hydrated in water. Occasionally, helical ribbons are observed which appear to be right handed (Figure 9 (left)). This small helical ribbon is only 0.125 μm in width. Figure 9 (right) shows the hollow tubules typical for this aldonamide. The micrographs show the internal and external helical markings on the tubules demonstrating their likely helical precursors. The width of the helical ribbons is between 0.2–0.3 μm with an overall tubular diameter of 0.1 μm.

The pentose aldonamide, *N*-dodecyl-L-lyxonamide, and the tetrose, *N*-dodecyl L-threonamide form morphologies similar to their diacetylenic analogs. These L-lyxonamide tubules exhibit a high aspect ratio and appear to be formed by the rolling up of planar sheets. The tubules have diameters around 0.4 μm, which are much smaller than the diacetylenic analog. The saturated L-threonamide is a flat crystalline assembly with some irregular surface topology.

The saturated aldonamides do not all form supramolecular assemblies similar to their diacetylenic analogs. The *N*-dodecyl-D-gluconamide forms twisted ropelike or braided fiber assemblies when hydrated in water compared to the planar multilayer sheets from the diacetylenic analog. A similar morphology was observed by Fuhrhop and co-workers for the *N*-octyl-D-gluconamide.[16,17,23] The morphologies of the *N*-dodecyl D-galactonamide and *N*-dodecyl L-mannonamide were also similar to those reported for the corresponding *N*-octyl aldonamides.[17] Figure 10 shows braided fibers which are linked to larger aggregates. These aggregates appear to fuel the growth of the small fibers. High magnification of these materials suggests that they are formed by the twisting together of smaller fibers to give the ropelike appearance of these

(23) Köning, J.; Boettcher, C.; Winkler, H.; Zeitler, E.; Talmon, Y.; Führhop, J.-H. *J. Am. Chem. Soc.* **1993**, *115*, 693–700.

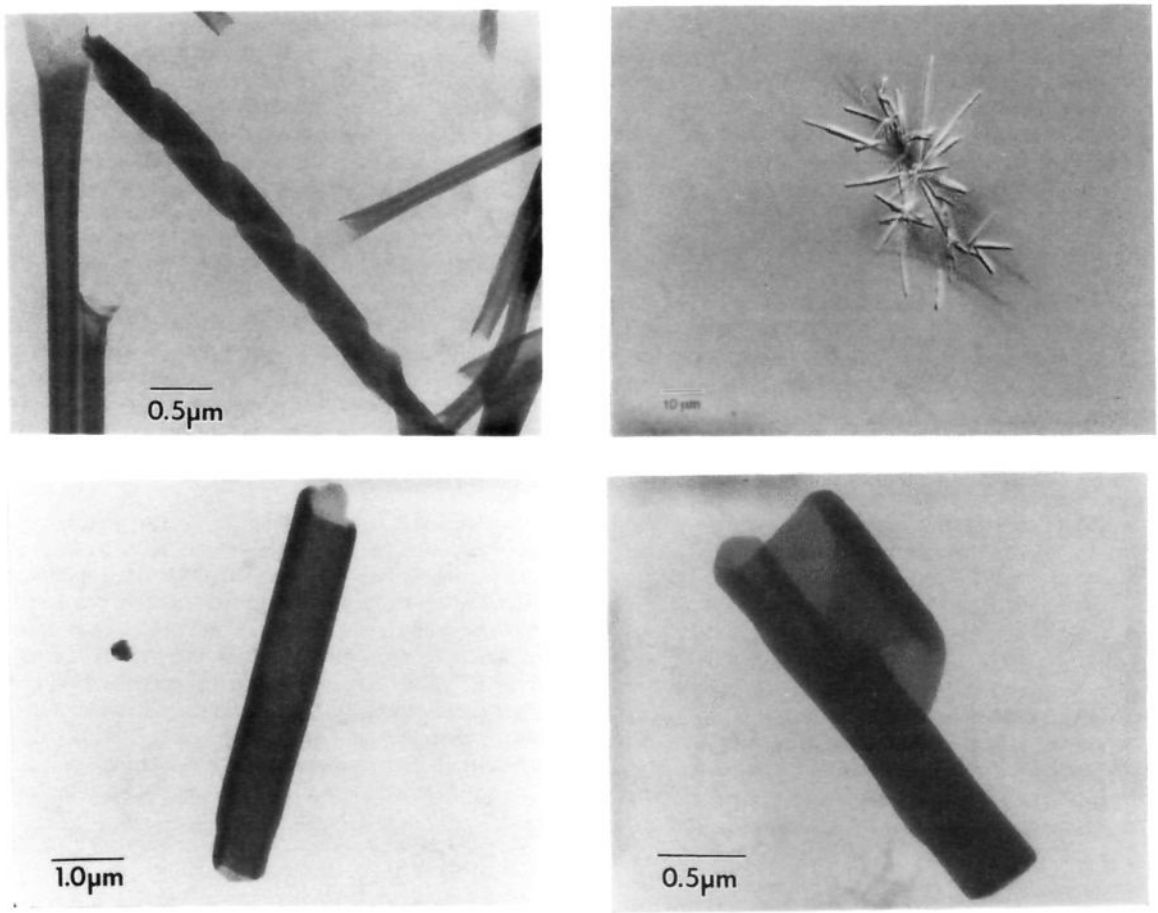

Figure 5. (Top left) TEM of unstained hydrated assemblies of *N*-dodeca-5,7-diynyl D-glycero-L-mannonamide. The helical structures comprise about 50% of the assemblies with the remainder appearing as tubules (1.0 mg lipid/mL water). (Top right) video-enhanced optical micrograph of assemblies of *N*-dodeca-5,7-diynyl D-glycero-L-mannonamide show that the morphology is the same in an aqueous environment as in the dried state (1.0 mg lipid/mL water). (Bottom left) TEM of assemblies of polymerized *N*-dodeca-5,7-diynyl L-mannonamide (0.25 mg lipid/mL water). (Bottom right) TEM of a partially unwound *N*-dodeca-5,7-diynyl L-mannonamide assembly (1.0 mg lipid/mL water).

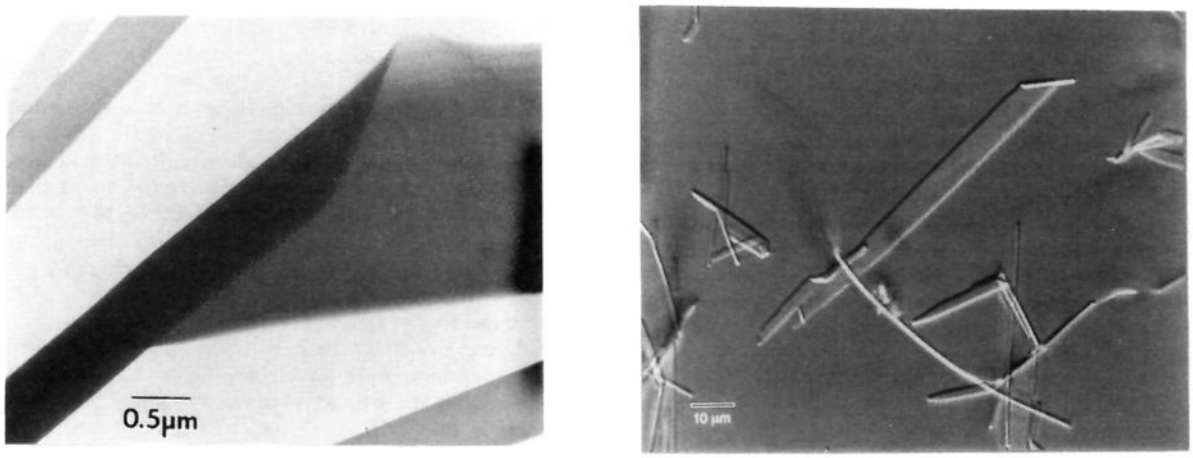

Figure 6. Supramolecular assemblies of unstained hydrated *N*-dodeca-5,7-diynyl L-lyxonamide. (Left) TEM showing bilayer sheets and tubules (1.0 mg lipid/mL water). (Right) video-enhanced optical micrograph.

assemblies. The individual fibers are 12–15 nm in diameter forming a twisted rope with an overall diameter of nearly 40 nm.

The *N*-dodecyl-L-arabonamide assembly is also significantly different from the diacetylenic analog. The morphology of the saturated aldonamide is tubular (Figure 11 (left and right)). The hollow center of the tubule is apparent as the dark stained area which runs the entire distance of the assembly. The open end of the tubule shows evidence of the multilayers which make up the assembly. The diameter of the tubules varies from 0.4 to 0.7 μm. This is smaller than the other saturated aldonamide tubules but about twice the size of diacetylenic tubules.

Discussion

The assembly of both the saturated and diacetylenic aldonamides into nonspheroidal morphologies provides novel materials for micro or nanofabrication.[6] Considerable interest in tubular microstructures has been generated by the extensive

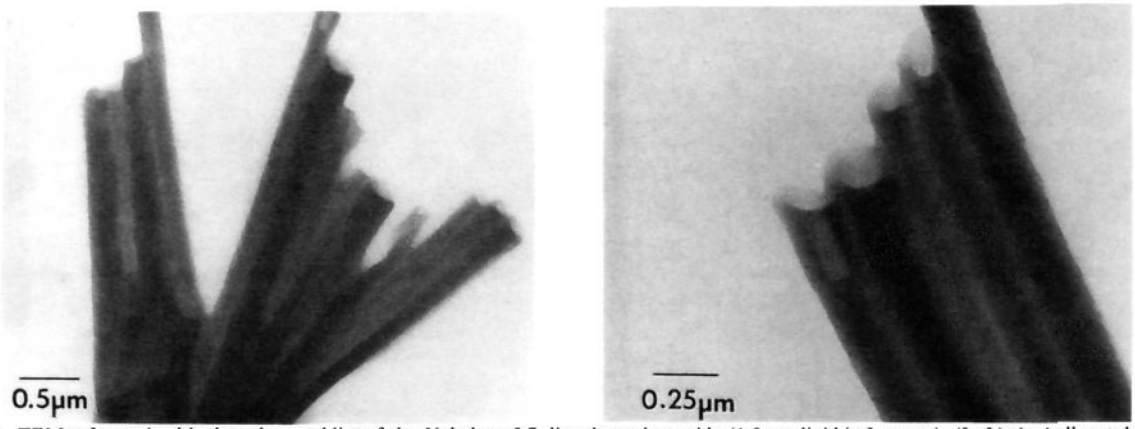

Figure 7. TEMs of unstained hydrated assemblies of the *N*-dodeca-5,7-diynyl D-gulonamide (1.0 mg lipid/mL water). (Left) the hollow tubules are formed from the twisting of smaller structures. (Right) the tubules aggregate to form "log jams" as shown in the enlargement (1.0 mg lipid/mL water).

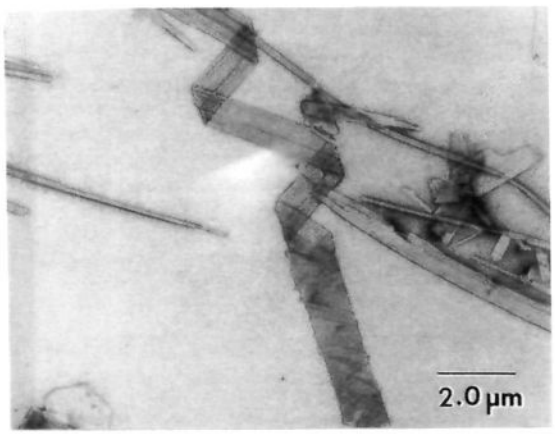

Figure 8. TEM of stained hydrated assemblies of *N*-dodecyl-D-galactonamide. The saturated galactonamide is more fragile than the diacteylenic D-galactonamide and collapses upon dehydration (1.0 mg lipid/mL water). Sample stained with 0.5% PTA.

studies of $DC_{8,9}PC$ at the Naval Research Laboratories.[24] Numerous potential applications of $DC_{8,9}PC$ tubules have been proposed.[25] These include the sustained release over several months of reagents from the hollow tubule interior. The release rate is dependent on the molecular characteristics of the reagent as well as the length and internal diameter of the tubule. Several of the aldonamides described here readily form tubules. Diacetylenic aldonamides, i.e., galactonamide, glyceromannonamide, mannonamide, and lyxonamide, and some saturated dodecyl aldonamides, i.e., galactonamide, mannonamide, arabonamide, and lyxonamide, were observed to form tubules. The tubules from diacetylenic aldonamides ranged from ca. 0.3 to 0.4 μm in diameter, which is similar to that reported for the $DC_{8,9}PC$ tubules. In contrast, the tubules from dodecyl galactonamide and mannonamide were about three times larger in diameter. Each class offers interesting opportunities for reagent encapsulation and release. The relative ease of preparation of many of the aldonamide molecules and their hydrated assemblies recommends them for applications that require large amounts of amphiphile.

In spite of the morphological similarities of the assemblies formed by $DC_{8,9}PC$ and some aldonamide amphiphiles, there are some striking differences. The propensity of some saturated alkyl aldonamides to form tubules clearly demonstrates that the incorporation of a diacetylenic group into the hydrophobic tail(s) of the amphiphiles is not requisite for tubule formation. Aldonamide tubules formed from nonpolymerized amphiphiles are robust during sample handling for electron microscopy. TEM requires drying the samples which can result in deformation of the assemblies. Early TEMs of $DC_{8,9}PC$ tended to show collapsed helical and tubule microstructures. Freeze fracture electron microscopy and premetalization of $DC_{8,9}PC$ tubules were usefully employed to preserve the tubule morphology during microscopy.[11,25] The *N*-dodecyl-D-galactonamide TEMs show evidence of sample collapse. But the dodecylmannonamide, arabonamide, and lyxonamide appear as unperturbed helical or tubular structures in the micrographs. These data may be indicative of the relative strengths of the hydrogen bonding in these different assemblies, but further studies are necessary to test this hypothesis.

The diacetylenic aldonamides assemblies are also robust. In most of the TEMs of helical and tubular microstructures, the morphology appears to be unperturbed by the drying process. Again the intermolecular forces are sufficiently strong to resist collapse of the three-dimensional morphology. This appeared to be true whether the samples were or were not photopolymerized before TEM preparation. Of course, the facile polymerization of these diacetylenic aldonamides may permit their partial polymerization during electron microscopy. However, we noted that prepolymerized samples for TEM were always more highly colored after microscopy than the nonphotopolymerized aldonamide samples.

The topotactic polymerization diacetylenes occurs in an efficient manner only when the diacetylene groups are well-ordered as found in a crystalline lattice or a bilayer in the solid analogous phase. The absorption characteristics of polydiacetylene formed from an assembly of monomers is related to the effective conjugation length of the polymer, which is an indirect measure of the order in the assembly prior to polymerization. We observed that the diacetylene reactivity in each of the aldonamide series is greatest for the heptoses and hexoses. Therefore, changes in headgroup size affect the assembly morphology, as well as the packing arrangement of the chains. This could be due to a small translation in the *y*-direction of the assembly. Photopolymerization of tubules from diacetylenic galactonamide, glyceromannonamide, and mannonamide rapidly produced blue to blue-purple polydiacetylenes (PDAs) at high conversion.[20,26] This is in sharp contrast with the polymerization of $DC_{8,9}PC$ which gives red PDA in relatively low yield. Photopolymerization to yield PDA assemblies has been shown to increase their solvent stability.[20] The unpolymerized tubules from diacetylenic galactonamide can be disrupted by hydrogen-bonding solvents such as formamide. The photopolymerized tubules were not dissolved by formamide or DMSO, but were merely dispersed. Thus, the polymerization of assemblies from the diacetylenic aldonamides produce microstructures that can be handled in some organic solvents as well as water.

(24) Schnur, J. M. *Science* **1993**, *262*, 1669–1676.
(25) Schnur, J. M.; Price, B.; Schoen, P. E.; Yager, P.; Calvert, J. M.; Georger, J.; Singh, A. *Thin Solid Films* **1987**, *152*, 181–206.
(26) Frankel, D. A.; O'Brien, D. F. *Macromol. Sym.* **1994**, *77*, 141–148.

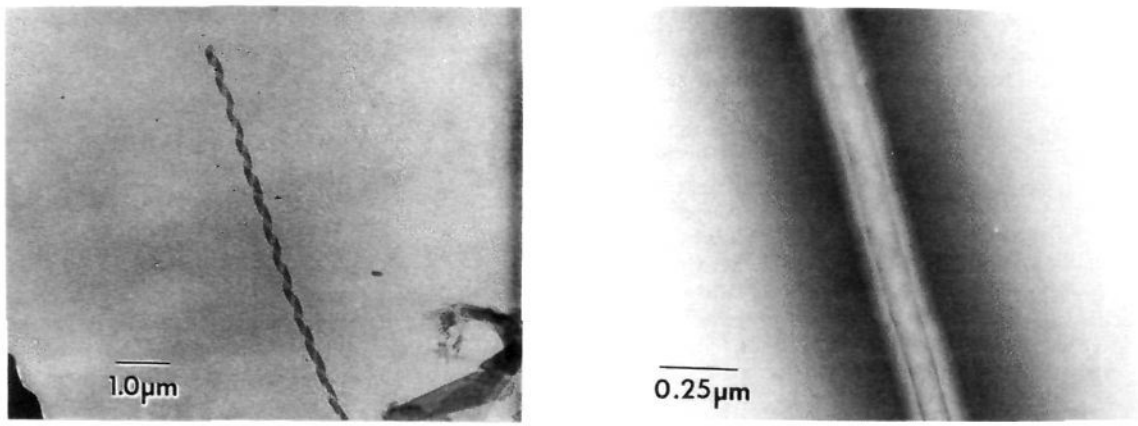

Figure 9. TEMs of stained hydrated assemblies of *N*-dodecyl-L-mannonamide (1.0 mg lipid/mL water). (Left) sample stained with 0.5% PTA. (Right) hollow tubule with helical markings on the outside of the tubule and along the inner aqueous core. Sample stained with 1% UA.

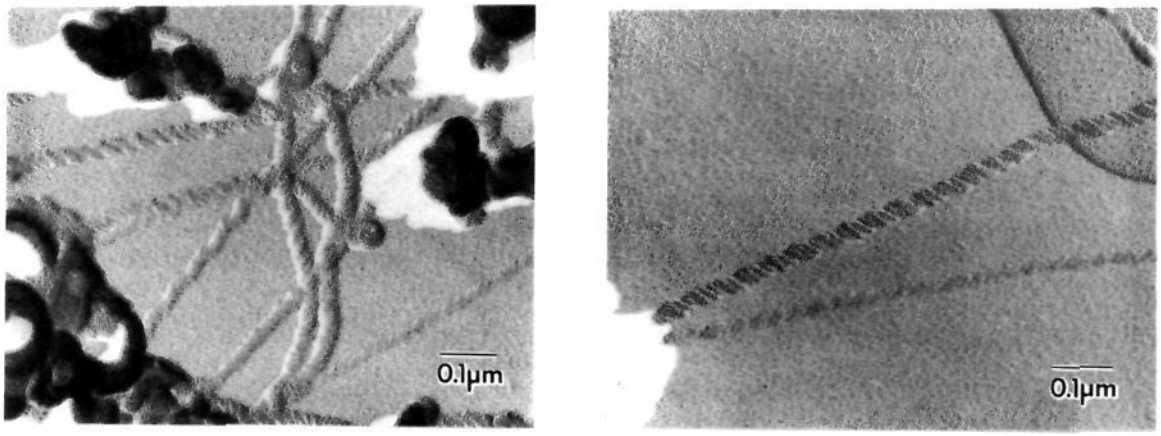

Figure 10. TEMs of shadowed hydrated assemblies of *N*-dodecyl-D-gluconamide (1.0 mg lipid/mL water). The braided structure appears to be composed of several interwinding strands. Samples shadowed with platinum at angle of 35°.

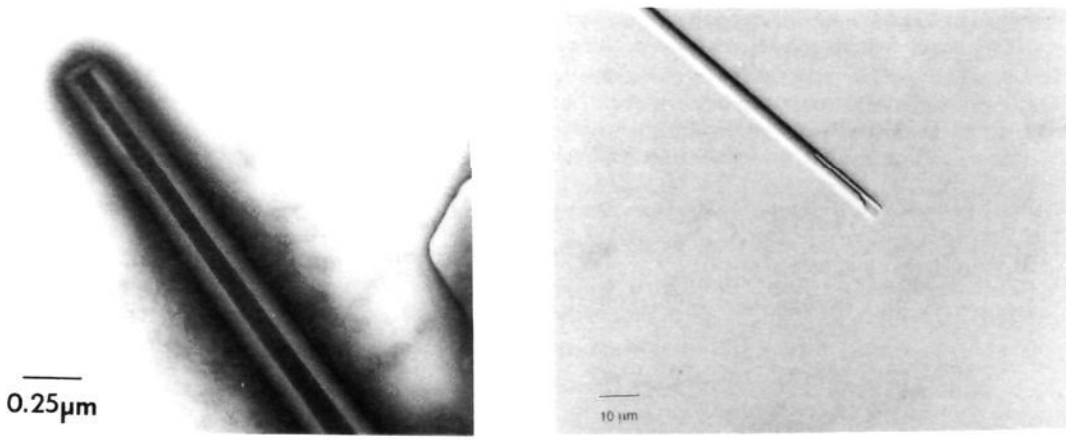

Figure 11. (Left) TEM of stained hydrated assemblies of *N*-dodecyl-L-arabonamide. The hollow tubule is strikingly different from the braided structure of its diacetylenic analog (see Figure 3) (1.0 mg lipid/mL water). Sample stained with 1% UA. (Right) video-enhanced optical micrograph of *N*-dodecyl L-arabonamide assemblies (1.0 mg lipid/mL water).

The relationship between molecular structure and supramolecular morphology in instances where nonspheroidal structures are preferentially formed is poorly understood. This is due in part to the lack of a systematic approach to the modification of amphiphile structure. Here we have systematically varied the aldonamide headgroup in order to evaluate the contribution of head group interactions to assembly morphology. Furthermore, as discussed next, these experimental observations have been compared to predicted hydrogen bonding patterns in order to develop an initial model for the aggregation behavior of *N*-alkylaldonamides.

Since we have been unable to crystallize any of the diacetylenic aldonamides in either a hydrated or unhydrated state, a molecular modeling approach was adopted to examine the probable intermolecular hydrogen bonding patterns and to compare these predicted patterns to the observed morphology. The molecular modeling of the diacetylenic aldonamides is complicated by the numerous possible conformations of a single aldonamide. A conformational search that only allowed rotation of the C–C bond and C–O bonds of the sugar would yield an enormous number of minimum energy conformations, many of which differ by less than 1 kcal/mol. There are also a fair number of conformations

that form *intra*molecular hydrogen bonds. But such bonding is unlikely in an extended array (bilayer or monolayer lattice) of these amphiphiles. Therefore, it is important to extend the model from a single amphiphile to an array of molecules. Constraints on the possible structures can be obtained from either solid state NMR or diffraction data, as has been reported for fibers of *N*-octyl-D-gluconamide.[27] However, these type of data are not currently available for diacetylenic aldonamides. Therefore, the modeling described below is an initial study to examine the relevance of headgroup size and stereochemistry on the hydrogen bonding patterns and energy of some assemblies. This approach has revealed some factors of apparent importance to the formation of various types of supramolecular morphologies.

The amphiphiles were modeled based on the aldonamide structures reported in the Cambridge X-ray crystallographic database. A search of the Cambridge crystallographic database provided nine structures incorporating D-gluconamides with various alkyl tails: *N*-heptyl,[28] *N*-octyl,[29] *N*-decyl,[28] *N*-undecyl,[30] *N*-benzyl,[31] *N*-cyclohexyl,[32] *N*-(2-chloroethyl),[33,34] and *N*-isopropyl.[35] One pentose aldonamide, *N*-decyl-D-ribonamide, was also found.[36-38] An additional structure, *N*-octyl-D-talonamides, has recently been reported.[39] A related set of amphiphiles includes the 1-deoxy-1-(*N*-methylalkanamido)-D-glucitols which differ from the *N*-alkylaldonamides in the methylated amide nitrogen. These compounds are excellent detergents for protein solubilization and do not form gels with tubular and helical morphologies. The compounds having an odd number of carbon atoms in the alkyl chains exhibit head-to-tail molecular packing.[40,41] When the chain is even numbered, the molecular packing is the bilayer head-to-head pattern, which is also observed for the *N*-alkylpyranosides and in related structures such as triacetyl- and glycosyl-phytosphingosines.[42]

X-ray crystallographic data of *N*-alkylaldonamide assemblies is limited to these headgroups: D-glucose, D-gulose, D-ribose, and D-talose. Since the data are for nonhydrated crystals rather than hydrated supramolecular assemblies they must be used with caution. Despite this drawback, these data provide a correlation between molecular packing, probable hydrogen bonding patterns, and the type of supramolecular morphology exhibited (Table 2).

The *N*-alkyl D-gluconamides all exhibit complex cyclic hydrogen bonding patterns of the sugar hydroxyls in addition to intermolecular amide hydrogen bonding.[29] The typical hydrogen bonding is a four-molecule homodromic cycle. This homodromic hydrogen bonding pattern (cyclic bonding pattern where the donor acceptors are unidirectional) link together four amphiphiles using all the available donor–acceptor pairs in the headgroup. The absence of free hydroxyls on the sugar headgroup allows the amphiphile to pack in an unusual head-to-tail orientation, which resembles a crystal more than a typical bilayer. This feature of the crystal structure is common to all the *N*-alkylgluconamide structures reported, irrespective of the difference in crystal symmetry between those with even- and odd-numbered atoms in the alkyl chains.

Table 2. Hydrogen Bonding and Amphiphile Packing Patterns Obtained from the X-ray Crystallographic Data of Saturated *N*-Alkylaldonamides

headgroup	H-bonding pattern	amphiphile packing	morphology
D-glucose	homodromic	head-to-tail	braided fibers
D-ribose	homodromic	head-to-tail	NA
D-talose	interbilayer	head-to-head	sheets
D-gulose	interbilayer	head-to-head	sheets

The crystallographic search provided invaluable conformational information for several *N*-alkyl-D-gluconamides which were similar to our amphiphiles. A consistent finding was head-to-tail amphiphile packing with a linear glucose headgroup despite a 1,3-syndiaxial hydroxyl interaction. When the fatty acids were long, compounds with even and odd numbers of carbon atoms in the chains gave different crystal structures. Apparently, the intricate interglucose hydrogen bonding is the underlying basis for the observed crystal packing. This is probably because the favored all-trans form of the D-gluconamide moiety positions the OH and amide groups in well-defined orientations. This arrangement determines the formation of intermolecular hydrogen bonds between OH and amide groups, which must be stronger than the van der Waals interactions of the alkyl chains.[28-30]

The crystallographic data for *N*-decyl-D-ribonamide are similar to that of the D-gluconamides.[36] The ribonamide packs in a head-to-tail orientation with a homodromic hydrogen bonding cycle. The supramolecular morphology of this hydrated aldonamide remains to be reported. The *N*-decyl-D-ribonamide, although different from *N*-decyl-D-gluconamide in the stereochemistry and size of the sugar headgroup, are also arranged head-to-tail. The decyl chain is in an extended all-trans conformation and all the C–C–C–C torsional angles are close to 180°. Strong hydrogen bonding via the amide linkage exists through parallel planes with a four molecule homodromic hydrogen bonding cycle.[36] The homodromic cycle is perpetuated through four molecules with coordinates (x, y, z), $(x + 1, y, z)$, $(x, y + 1, z)$, and $(x, y, z + 1)$.

The crystallographic data for *N*-octyl-D-gulonamide[43] and for *N*-octyl-D-talonamides[39] do not show the cyclic hydrogen bonding cycle observed for the other two amphiphiles. The available headgroup donor–acceptor pairs permit an interbilayer hydrogen bonding scheme that yields planar morphologies.

The assembly of a collection of amphiphiles into a particular supramolecular morphology is a consequence of their molecular structure and the dominant noncovalent interactions, including van der Waals forces, hydrophobic effect, dipolar forces, and hydrogen bonding. Aldonamides, when hydrated in water at elevated temperatures, form micelles.[8] Upon cooling through the phase transition temperature, the micelles convert to nonspheroidal morphologies. The major change in noncovalent interactions upon loss of thermal energy is most likely the formation of additional hydrogen bonds between amphiphiles and between the assembly surface and water.

Fuhrhop et al. explained the preferred morphology of saturated aldonamides of selected hexoses by consideration of both the

(27) Svenson, S.; Köning, J.; Fuhrhop, J.-H. *J. Phys. Chem.* **1994**, *98*, 1022–1028.
(28) Muller-Fahrnow, A.; Hilgenfeld, R.; Hesse, H.; Saenger, W.; Pfanemuller, B. *Carbohydr. Res.* **1988**, *176*, 165–174.
(29) Zabel, V.; Muller-Fahrnow, A.; Hilgenfeld, R.; Saenger, W.; Pfannemuller, B.; Enkelman, V.; Welte, W. *Chem. Phys. Lipids* **1986**, *39*, 313–327.
(30) Jeffrey, G. A.; Makuszynska, H. *Carbohydr. Res.* **1990**, *207*, 211–219.
(31) Oddon, Y.; Darbon-Meyssonnier, N.; Reboul, J. P.; Pepe, G.; Decoster, E.; Pavia, A. A. *Acta. Crystallogr.* **1986**, *C42*, 1764–1766.
(32) Darbon, P. N.; Odden, Y.; Lacombe, J. M.; Decoster, E.; Pavia, A. A. *Acta. Crystallogr.* **1984**, *C40*, 1105–1107.
(33) Statzke, L. O. G.; Mackay, M. F. *Acta. Crystallogr.* **1975**, *B31*, 1128–1132.
(34) Sindt, A. C.; Mackay, M. F. *Acta. Crystallogr.* **1977**, *B33*, 2659–2662.
(35) Darbon-Meysonnier, N.; Oddon, Y.; Decoster, E.; Pavia, A. A. *Acta. Crystallogr.* **1985**, *C41*, 1324–1327.
(36) Tinant, B.; Declercq, J. P.; Van Meerssche, M. *Acta Crystallogr.* **1986**, *C42*, 579–581.
(37) Baeyens-Volant, D.; Fornasier, R.; Szalai, E.; David, C. *Mol. Cryst. Liq. Cryst.* **196**, *135*, 93–110.
(38) Baeyens-Volant, D.; Cuvelier, P.; Fornasier, R.; Szalai, E.; David, C. *Mol. Cryst. Liq. Cryst.* **1985**, *128*, 277–286.
(39) Andre, C.; Luger, P.; Svenson, S.; Fuhrhop, J.-H. *Carbohydr. Res.* **1993**, *240*, 47–56.
(40) Jeffrey, G. A.; Maluszynska, H. *Acta. Crystallogr.* **1989**, *B45*, 447–452.
(41) Muller-Fahrnow, A.; Zabel, V.; Steifa, M.; Hilgenfeld, R. *J. Chem. Soc. Chem. Commun.* **1986**, 1573–1574.
(42) Jeffrey, G. A. *Accs. Chem. Res.* **1986**, *19*, 168–173.
(43) Andre, C.; Luger, P.; Svenson, S.; Fuhrhop, J.-H. *Carbohydr. Res.* **1992**, *230*, 31–40.

conformation of the sugar headgroup and the overall shape of the molecule.[17] The sugar headgroup of *N*-octyl-D-galactonamide can adopt an all-trans conformation; thus, the molecule can assume a linear cylindrical shape that readily forms a bilayer arrangement. Bilayer sheets can roll up or twist in a variety of ways to form nonspheroidal morphologies. If one end of the bilayer sheet is held fixed and the other end twisted, a helical structure results. The helix can twist tighter to form hollow tubules with helical markings on both the inside and outside of the assembly. The bilayer sheet can also roll up perpendicular to one edge to form a hollow tubule. Examination of the open end of the tubule shows the concentric bilayer sheets from which it is formed. Finally, the bilayer sheet can be rolled up from an edge to form a hollow tubule which can also exhibit helical markings on both surfaces.

On the other hand, the 1,3-syndiaxial interactions of the sugar hydroxyls of an aldonamide such as *N*-octyl-D-gluconamide causes a 120° rotation of the C–C bond, resulting in a bent molecular conformation, which does not readily aggregate into an amphiphilic bilayer. Instead the gluconamide assumes a wedge shape and adopts a micellar arrangement.[17] In this model the "wedges" aggregate in a manner that maximizes intermolecular hydrogen bonding and results in formation of micellar rods. The rods form fibers with high aspect ratios which then twist or braid together to form the observed braided fiber assemblies.

Due to the limited crystallographic data of aldonamides having differing headgroups, it is not yet possible to predict molecular packing and the hydrogen bonding arrangements of the diacetylenic aldonamides described here. Therefore, the aldonamides were divided into two distinct parts, the variable headgroup and the constant acyl chain. Molecular modeling focused primarily on the variable sugar headgroups. This allowed the development of a model based on the large amount of information available from the X-ray crystal structures of the alditols. The alditols are similar to the aldonamide sugar headgroups in that they are open chain, contain the same configuration, and can rotate around C–C and C–OH bonds. However, the alditols terminus is a CH_2-OH moiety, whereas the aldonamides contain an amide linkage to the rest of the molecule. The alditols pack together in crystals to maximize intermolecular hydrogen bonding which includes all of the donor–acceptor pairs in the molecule. This causes perturbations in the conformation of the alditols which are not apparent in the aldonamide literature.

A comparison of the conformations of D-glucitol and D-ribitol directly illustrates this point. The X-ray crystal structures of several alditols have been reported including D-glucitol and D-ribitol. In all cases studied to date, the alditols pack in an all-trans zig–zag conformation when there are no 1,3-syndiaxial interactions.[44] This is the case for galactitol, arabinitol, and mannitol. If such a 1,3-syn hydroxy interaction is possible, then the carbon chain adopts a nonlinear, or bent, chain conformation to minimize these interactions by a 120° rotation about a C–C bond (Figure 12).[44] This "rule" has been demonstrated with numerous alditols and successfully used to predict the conformation of alditols that were later characterized by X-ray crystallography.

The unique packing of these amphiphiles and the lack of additional X-ray data make it impossible to "predict" a set of rules to model the diacetylenic aldonamides. In spite of these limitations, the modeling protocol, as described in the Experimental Section, was useful in demonstrating the ability of these amphiphiles to pack in different arrangements based upon differences in the stereochemistry and size of the headgroups. The modeling results showed a variation in molecular packing, energy of the lattice, and hydrogen bonding patterns. Emphasis was placed on the different arrangements of hydrogen bonding patterns.

(44) Jeffrey, G. A.; Kim, H. S. *Cabohydr. Res.* **1970**, *14*, 207–216.

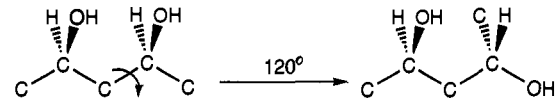

Figure 12. Conformations of alditols with 1,3-syndiaxial interactions.

In order to test the ability of the modeling protocol to accurately predict hydrogen bonding cycles, both *N*-octyl-D-gluconamide and the *N*-decyl-D-ribonamide were subjected to the modeling protocol. The X-ray crystallographic data for these compounds and the modeling data obtained by using the alditol headgroup were compared. Our modeling protocol successfully predicted the hydrogen bonding cycles of these aldonamides when the conformation of the aldonamide was based on the alditol crystal structure to build the 2 × 2 lattice. The hydrogen bonding patterns were compared and found to be nearly identical to those from the aldonamide crystal structure analysis. This result is encouraging since the modeling is based on the lowest energy of interaction of the molecules in the lattice, as generally expected for the crystal structure. The hydrogen bonding patterns and lengths are shown for both the molecular modeling lattice and the X-ray lattice for *N*-octyl-D-gluconamide (Figure 13). Both hydrogen bonding patterns contain a two-molecule, three-donor/acceptor homodromic hydrogen bonding cycle and have similar hydrogen bond lengths. The hydrogen bond lengths are comparable for the intermolecular hydrogen bond between the terminal oxygen donor $O_{(6)}$ and the hydrogen on $O_{(5)}$. The most significant difference is the bifurcated carbonyl hydrogen bond associated with the Sybyl modeled lattice which is not present in the X-ray crystal structure. This links together the homodromic cycle to the amide hydrogen bond in a finite chain and lowers the energy of this lattice relative to the X-ray crystallographic data.

This experiment illustrates that the modeling protocol can reasonably predict the experimentally determined lattice structure and hydrogen bonding patterns of these compounds. The same hydrogen bonding patterns were observed by both methods, plus some additional hydrogen bonds were predicted by the Sybyl model. It should also be noted that the hydrogen bond lengths obtained for the two techniques vary slightly. The assumption that the alditol X-ray structure is the same as the corresponding aldonamide depends on a preference for straight chain conformations.

The predicted hydrogen bonding patterns for the diacetylenic D-galactonamide series are depicted in Figure 14. These hydrogen bonding schemes vary significantly among the amphiphiles in this series. All three of these compounds show strong interplanar amide hydrogen bonding along parallel sheets of amphiphiles. The L-threonamide has a bifurcated amide bond with the carbonyl ($O_{(1)}$) oxygen simultaneously donating to the amide hydrogen and to the hydrogen on $O_{(2)}$. The L-threonamide has a simple hydrogen pattern in addition to the bifurcated amide bond. The intermolecular hydrogen bonding pattern links the amphiphiles in parallel sheets. Here, $O_{(3)}$ is hydrogen bonded to hydrogen on $O_{(4)}$ of the amphiphile translated one unit in the *y*-direction. The D-galactonamide's hydrogen bonding pattern is quite simple with an intramolecular hydrogen bond between $O_{(3)}$ and the hydrogen on $O_{(2)}$. The L-arabonamide displays a four-molecule antidromic hydrogen cycle. The cycle links four amphiphiles related to each other by simple translations in the *x*, *y*, or *z* directions. This cycle is antidromic in nature but is very similar to the homodromic cycle reported for the *N*-alkyl-D-gluconamides.[28-30]

The number of donor–acceptors pairs involved in the hydrogen bonding patterns varies significantly with the molecular structure. Whereas the D-galactonamide and L-threonamide each use only two of the oxygen donors, the L-arabonamide uses all five. Therefore, the L-arabonamide is unable to hydrogen bond through $O_{(5)}$ to water or another layer of amphiphiles, and would be expected to pack only in a head-to-tail fashion. This type of

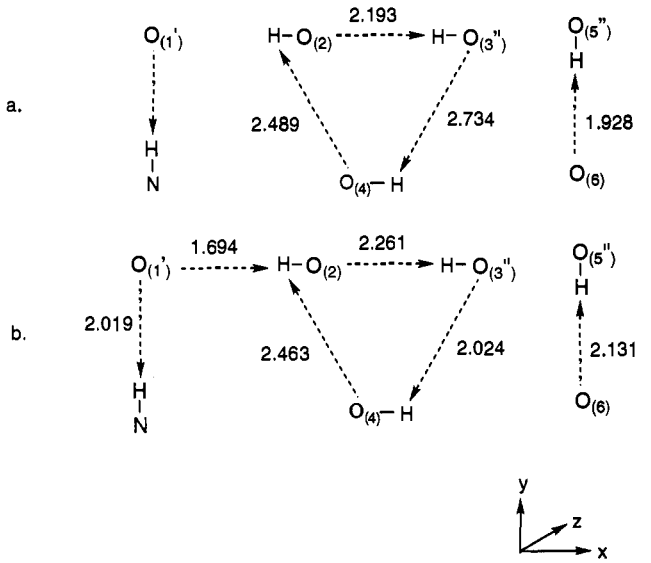

Figure 13. Comparison of hydrogen bonding patterns by two different modeling techniques of *N*-octyl-D-gluconamide: (a) X-ray crystal lattice (FAKFUS) and (b) modeling of the lattice by Sybyl. The key to the atom labeling is: $' = x, y + 1, z$, $'' = x, y + 1, z + 1$, $''' = x, y + 2, z + 1$. Hydrogen bond lengths given in Å.

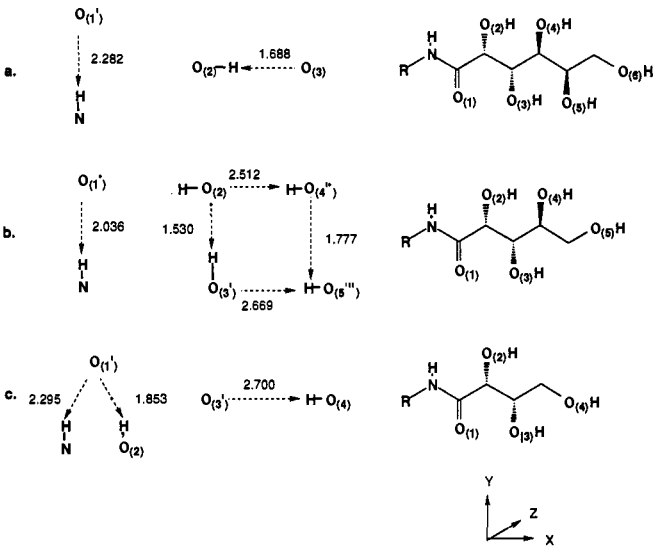

Figure 14. Hydrogen bonding patterns for the diacetylenic D-galactonamide series: (a) D-galactonamide, (b) L-arabonamide, and (c) L-threonamide. The amphiphiles are translated one arbitrary unit in x, y, and z as follows: $' = x, y + 1, z$, $'' = x, y, z + 1$, $''' = x, y + 1, z + 1$. Hydrogen bond lengths given in Å with atom numbering given by subscripts.

orientation appears critical to the observed braided fiber supramolecular morphology. In the L-arabonamide, the supramolecular assembly appears to be made up of fiber structures, which is very similar to the ropelike morphologies observed by Fuhrhop and co-workers for the *N*-alkyl-D-gluconamides.[16,17] The other aldonamides in this series have hydroxyl groups free to participate in interlayer hydrogen bonding, which ultimately leads to head-to-head bilayer packing arrangements. This suggests that the hydrogen bonding pattern controls the packing arrangements and possible the supramolecular morphologies of each of these aldonamides.

Only one of the modeled diacetylenic aldonamides, the L-arabonamide, appears to exhibit a "dromic" hydrogen bonding cycle. The validity of the antidromic hydrogen bonding cycle found in the diacetylenic L-arabonamide was tested further. The diacetylenic chains of the amphiphile were removed and replaced with saturated (C_{12}) tails in the 2 × 2 lattice. The lattice energy was then reminimized in the TRIPOS force field and resultant hydrogen bonding was no longer an antidromic hydrogen bonding cycle (Figure 14b) but a less complicated pattern (Figure 15). The supramolecular morphologies of these assemblies are consistent with the predicted hydrogen bonding patterns. The antidromic cycle associated with braided fiber assembly of the diacetylenic L-arabonamide changed to a simpler pattern consistent with the bilayer tubule morphology for the *N*-dodecyl-L-arabonamide.

The predicted hydrogen bonding patterns for the L-mannonamide series (Figure 16) vary significantly, but without involving the primary hydroxyl group. All three of these amphiphiles in this series have bifurcated hydrogen bonds emanating from the carbonyl oxygen. The L-mannonamide and the D-erythronamide bifurcated hydrogen bonds start with the carbonyl donor with both acceptors on the amphiphile in the same plane. The L-lyxonamide's carbonyl oxygen intramolecularly hydrogen bonds with the hydrogen on $O_{(3)}$ as well as to the amide hydrogen on the neighboring amphiphile in the same plane. The L-mannonamide displays another cycle which links $O_{(2)}$, $O_{(4)}$, and $O_{(5)}$ in three different amphiphiles. The most significant difference in this series is the complex hydrogen bonding scheme for the L-mannonamide. In all three of these amphiphiles, terminal oxygen donors are available for interlayer hydrogen bonding, which enhances the probability of head-to-head packing. Neither

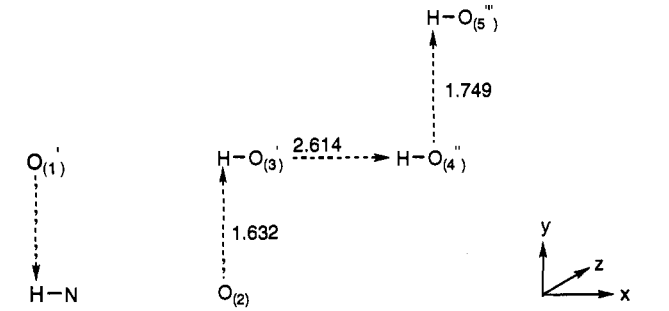

Figure 15. Molecular modeling of hydrogen bonding patterns of *N*-dodecyl-L-arabonamide. The key to the atom labeling is: $' = x, y + 1, z$, $'' = x, y + 1, z + 1$, $''' = x, y + 2, z + 1$. Hydrogen bond lengths given in Å.

the mannonamide nor the lyxonamide assembly forms rodlike morphologies as was the case for the head-to-tail packing *N*-alkyl-D-gluconamides or the diacetylenic L-arabonamide.

Although the relationship between molecular structure and supramolecular morphology of these aldonamides remains to be fully elucidated, the experimental data presented here suggests the headgroup conformation and hydrogen bonding arrangements play important roles. Linear sugar headgroups allow the amphiphiles to pack together in extended "bilayer" sheets which grow to a point where the balance of forces (dipolar, chiral bilayer packing, and edge effects) causes the curvature of the assembly to change. This can result in formation of planar sheets, helical strands, or hollow tubules. The other extreme, as seen with the compounds with multimolecule dromic hydrogen bonding cycles, is the braided fiber supramolecular morphology. Since there are no oxygens free to contribute to interlayer hydrogen bonding this is a feasible packing arrangement. The conjugative effect of the hydrogen bonding cycle permits exclusion of water from the interlayer space. The molecules pack together in a helical micellar rod which may be composed on multiple head-to-tail layers as proposed for *N*-octyl-D-gluconamide, which has a double micellar arrangement.[23]

In summary, the data indicate the following: (1) Two packing arrangements have been confirmed by X-ray analysis. One is the head-to-head "bilayer" packing typical of most amphiphilic molecules. The other is a head-to-tail arrangement which is akin to the X and Z type of Langmuir–Blodgett films. (2) The head-

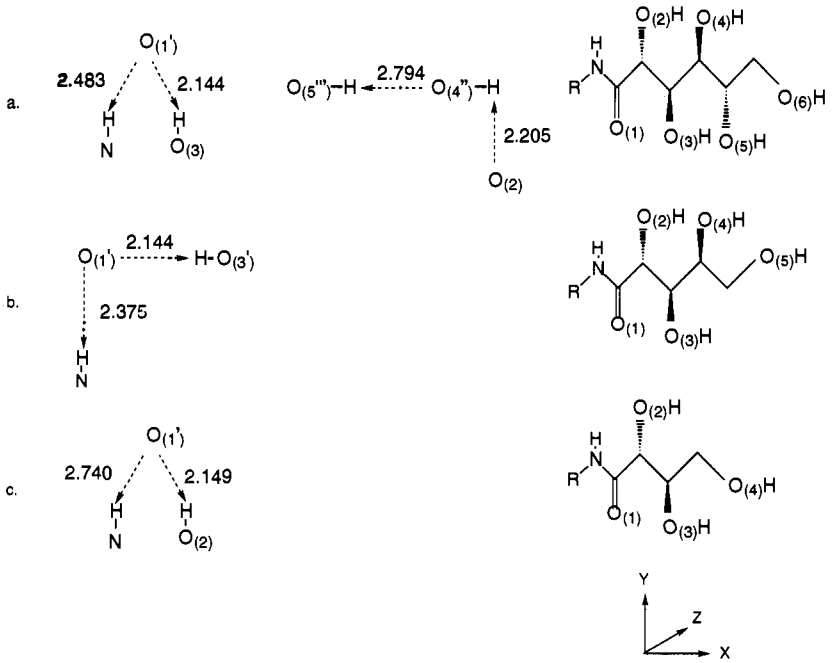

Figure 16. Hydrogen bonding patterns for the diacetylenic L-mannonamide series: (a) L-mannonamide, (b) L-lyxonamide, and (c) D-erythronamide. The amphiphiles are translated one arbitrary unit in x, y, and z as follows: $' = x, y + 1, z$, $'' = x, y, z + 1$, $''' = x, y + 1, z + 1$. Hydrogen bond lengths given in Å and atom numbering as subscripts.

to-tail packing arrangement and dromic hydrogen bonding patterns are associated with fiber-like supramolecular assemblies such as those observed in this study of aldonamides. Aldonamides that are associated through dromic hydrogen bonding patterns usually have no available oxygen donors for interlayer hydrogen bonds. (3) The head-to-head packing arrangement produces assemblies that are planar, helical, or tubular. The hydrogen bond patterns are simpler than those of the head-to-tail packing arrangement. All contain amide hydrogen bonding in parallel planes of molecules, but none of these lattices use all the available (especially terminal) oxygen donors; therefore, some oxygen donors are available to participate in interlayer hydrogen bonding. (4) The effects of the diacetylene group in the alkyl chains alters the packing of the headgroup such that the van der Waals distances between neighboring amphiphiles is larger. This small perturbation can alter the headgroup packing of the assembly, but the supramolecular morphology is altered only if this change is great enough to overcome the other intermolecular interactions.

Acknowledgment is made to the donors of the Petroleum Research Fund, administered by the American Chemical Society, for support of this research. The authors thank D. L. Bentley and B. Huey of the Electron Microscopy Facility, Division of Biotechnology, University of Arizona, for their assistance with the electron microscopy.

Supplementary Material Available: A listing of the synthesis and structural identification of the aldonamides and computer graphic images for the modeling summarized in Figures 14–17 (13 pages). This material is contained in many libraries on microfiche, immediately follows this article in the microfilm version of the journal, and can be ordered from the ACS; see any current masthead page for ordering information.